Comparative Bonding and Photophysical Properties of 2,2′-Bipyridine and 2,2′-Bipyrazine in Tetracyano Complexes Containing Ruthenium and Osmium

Mónica E. García Posse,[†] Néstor E. Katz,*[,†] Luis M. Baraldo,[‡] Diego D. Polonuer,[‡] Claudio G. Colombano,[‡] and José A. Olabe*[,‡]

Instituto de Química Física, Facultad de Bioquímica, Química y Farmacia, Universidad Nacional de Tucumán, Ayacucho 491, 4000 S. M. de Tucumán, República Argentina, and Departamento de Química Inorgánica, Analítica y Química Física, Inquimae, Facultad de Ciencias Exactas y Naturales, Universidad de Buenos Aires, 1428 Capital Federal, República Argentina

Received April 6, 1994[⊗]

The (2,2′-bipyrazine)ruthenium(II)− and (2,2′-bipyridine)osmium(II)−tetracyanide complexes were prepared as sodium and potassium salts, respectively. Assignments of the MLCT ($d\pi(M) \rightarrow \pi^*(L\text{-}L)$) and IL ($\pi(L\text{-}L) \rightarrow \pi^*(L\text{-}L)$) bands were performed analyzing spectra in aqueous solution and in organic solvents. Upon changing the solvent, we detected strong solvatochromic shifts, the energies of the MLCT bands going to lower values when the Lewis acidity of the solvent (measured by the Gutmann's acceptor number) was decreased. Redox potential values for the Ru(III,II) and Os(III,II) couples were also solvent-dependent, decreasing with the decrease in acceptor number. The basicities of coordinated cyanides toward the proton were measured through spectrophotometric titrations; the pK_a values so obtained, together with the IR measurements in the C−N stretching region (in solid samples and in organic solvents), and the potentials for ligand (L-L) reduction (in dimethylformamide solutions) were used as additional indicators of the $\sigma-\pi$ bonding interactions. Bipyrazine behaves as a stronger π-acceptor than bipyridine for a given metal center. On the other hand, for the same ligand environment, the Os(II) metal center behaves as a stronger π-donor compared to ruthenium and iron. The π-acceptor ability of the chelating ligand is enhanced in weakly acceptor solvents, associated with the changes in specific cyanide−solvent interactions. The complexes emit poorly in aqueous solutions at room temperature, with low quantum yields, as predicted by the potentials of the M(III,II) couples. The excited states are very strong reductants, as well as very weak oxidants.

Introduction

In view of the current interest in the spectroscopic, photophysical, and photochemical properties of metal−polypyridyl complexes,[1] the convenience of synthesizing substances with a single cromophoric unit has been emphasized. The studies on $[M(bpy)X_4]^n$ complexes (bpy = 2,2′-bipyridine) with M = Ru(II)[2] or Os(II)[3] showed that simpler spectra are obtained and that a tuning of excited state properties can be sought by a judicious variation in the nature of the nonchromophoric X ligands.[4−6]

The spectral and photophysical properties of the $[Ru(bpy)(CN)_4]^{2-}$ ion have been studied,[2,7] and the strong solvatochromism of the lowest energy MLCT band has been compared with that of other mixed Ru(II) complexes containing a variable number of coordinated cyanides.[8] Good correlations of the absorption and emission energies—as well as of the metal oxidation potentials—with the acceptor number of the solvent were obtained. On the other hand, no tetracyanide complexes of Os(II) with polypyridinic ligands have been prepared up to now.[9,10]

The spectral and photophysical properties of coordinated 2,2′-bipyrazine (bpz) have been studied in recent years;[11−14] as the studies on $[M(bpz)X_4]^n$ (M = Mo, W) complexes are limited to the X = CO compounds,[12,14,15] the synthesis of $[Ru(bpz)(CN)_4]^{2-}$ was also considered worthy.

The spectral (UV−vis, IR), electrochemical, and photophysical properties of the $[Ru(bpz)(CN)_4]^{2-}$ and of $[Os(bpy)(CN)_4]^{2-}$ complexes in aqueous and organic solvent solutions are reported here. The role of cyanides and the chromophoric ligands are discussed, with emphasis on the assessment of the back-bonding ability of each of the metals (Ru or Os) toward a particular ligand (bpy or bpz).

Experimental Section

Synthesis of the Complexes. (a) $Na_2[Ru(bpz)(CN)_4]\cdot 4H_2O$. The synthesis of the compound was similar to that previously described for the bipyridinic analogue;[2] 0.5 g of $K_4[Ru(CN)_6]\cdot 3H_2O$ (Alfa) and

* Telefax: 54-1-7820441. E-mail: olabe@inorba.uba.ar.
† Universidad Nacional de Tucumán.
‡ Universidad de Buenos Aires.
⊗ Abstract published in *Advance ACS Abstracts,* February 15, 1995.

(1) Juris, A.; Balzani, V.; Barigelletti, F.; Campagna, S.; Belser, P.; Von Zelewsky, *Coord. Chem. Rev.* **1988**, *84*, 85.
(2) Bignozzi, C. A.; Chiorboli, C.; Indelli, M. T.; Rampi Scandola, M. A.; Varani, G.; Scandola, F. *J. Am. Chem. Soc.* **1986**, *108*, 7872.
(3) Meyer, T. J. *Pure Appl. Chem.* **1986**, *58*, 1193.
(4) Kober, E. M.; Caspar, J. V.; Lumpkin, R. S.; Meyer, T. J. *J. Phys. Chem.* **1986**, *90*, 3722.
(5) Kober, E. M.; Marshall, J. L.; Dressick, W. J.; Sullivan, B. P.; Caspar, J. V.; Meyer, T. J. *Inorg. Chem.* **1985**, *24*, 2755.
(6) Kober, E. M.; Caspar, J. V.; Sullivan, B. P.; Meyer, T. J. *Inorg. Chem.* **1988**, *27*, 4587.
(7) Kato, M.; Yamauchi, S.; Hirota, N. *J. Phys. Chem.* **1989**, *93*, 3422.
(8) Timpson, C. J.; Bignozzi, C. A.; Sullivan, B. P.; Kober, E. M.; Meyer, T. J. Private Communication.
(9) Sharpe, A. G. *The Chemistry of Cyano Complexes of the Transition Metals*; Academic Press: New York, 1976; Chapter VII.
(10) Griffith, W. P. In *Comprehensive Coordination Chemistry*; Wilkinson, G., Gillard, R. D., Mc Cleverty, J. A., Eds.; Pergamon Press: Oxford, U.K., 1987; Vol. 4, Chapter 46.
(11) Crutchley, R. J.; Lever, A. B. P. *J. Am. Chem. Soc.* **1980**, *102*, 7128.
(12) Crutchley, R. J.; Lever, A. B. P. *Inorg. Chem.* **1982**, *21*, 2276.
(13) Haga, M. A.; Dodsworth, E. S.; Eryavec, G.; Seymour, P.; Lever, A. B. P. *Inorg. Chem.* **1985**, *24*, 1901.
(14) Dodsworth, E. S.; Lever, A. B. P.; Eryavec, G.; Crutchley, R. J. *Inorg. Chem.* **1985**, *24*, 1906.
(15) Ernst, S.; Kaim, W. *J. Am. Chem. Soc.* **1986**, *108*, 3578.

0020-1669/95/1334-1830$09.00/0

Table 1. Electronic Spectroscopic Data for $[Ru(bpz)(CN)_4]^{2-}$ and $[Os(bpy)(CN)_4]^{2-}$ Complexes, in Different Solvents[a]

$[Ru(bpz)(CN)_4]^{2-}$

solvent	AN	$(d\pi-\pi_1^*)^1$	$(d\pi-\pi_2^*)^1$	$(\pi-\pi_1^*)^1$	$(\pi-\pi_2^*)^1$
water	54.8	21.5 (5.7)	28.6 (6.0)	32.7 (26.0)	42.5 (14.0)
methanol	41.3	19.6 (5.7)	26.7 (6.3)	32.5 (22.5)	41.7 (20.5)
formamide	39.8	19.6 (6.7)	26.7 (7.2)	32.1 (26.5)	
1-propanol	37.3	19.0 (5.1)	25.6 (6.3)	32.3 (21.5)	42.0 (24.5)
ethanol	37.1	18.9 (6.2)	25.6 (7.7)	32.5 (26.0)	41.3 (14.0)
2-propanol	33.5	18.5 (5.0)	25.3 (6.8)	32.3 (20.0)	
dimethyl sulfoxide	19.3	16.9 (6.9)	23.5 (11.0)	32.1 (21.0)	
acetonitrile	18.9	17.7 (5.7)	24.4 (8.6)	32.5 (19.0)	42.0 (26.0)
dimethylformamide	16.0	17.2 (5.1)	23.5 (9.0)	32.1 (16.0)	
acetone	12.5	16.7 (5.0)	23.1 (9.8)		

$[Os(bpy)(CN)_4]^{2-}$

solvent	AN	$(d\pi-\pi_1^*)^3$	$(d\pi-\pi_1^*)^1$	$(d\pi-\pi_2^*)^1$	$(\pi-\pi_1^*)^1$	$(\pi-\pi_2^*)^1$
water	54.8	19.2 (0.40)	24.1 (1.9)		35.0 (13.5)	41.3 (7.1)
methanol	41.3	18.2 (0.50)	21.2 (1.6)	28.7 (2.1)	34.0 (12.0)	41.3 (5.8)
formamide	39.8	17.2 (0.55)	21.9 (2.1)	28.6 (2.3)	34.0 (15.0)	
1-propanol	37.3	16.7 (0.55)	21.2 (1.7)	28.7 (2.4)	34.0 (17.0)	41.3 (8.2)
ethanol	37.1	16.1 (0.60)	20.5 (2.0)	29.0 (2.9)	34.0 (17.0)	
2-propanol	33.5	15.1 (0.40)	20.0 (1.6)	27.8 (2.4)	34.0 (12.0)	
dimethyl sulfoxide	19.3	13.0 (0.50)	17.6 (2.2)	26.3 (3.6)	33.6 (15.0)	
acetonitrile	18.9	13.7 (0.45)	18.2 (1.9)	25.8 (3.8)	33.8 (11.0)	40.3 (8.6)
dimethylformamide	16.0	12.7 (0.50)	17.2 (2.1)	25.8 (3.8)	33.6 (14.0)	
acetone	12.5	12.8 (0.50)	17.0 (2.0)	25.0 (3.5)		

[a] Acceptor numbers (AN) are given according to Gutmann's scale.[26] Energy maxima ($\times 10^{-3}$) are in cm^{-1} ($\epsilon \times 10^{-3}$, $M^{-1}\ cm^{-1}$, in parentheses).

0.17 g of bpz (Aldrich) were dissolved in a 1:3 v/v mixture of methanol−water (34 mL) in a reaction flask. The original pale yellow solution was irradiated (under constant stirring) at 254 nm with a low-pressure Hg UV lamp for 52 h until the reaction was complete (unchanged spectrum). The solution was then filtered, and the filtrate was evaporated to dryness. The deep violet solid was dissolved in 5 mL of water, and the mixture was filtered to eliminate the excess of bpz; upon the addition of MeOH, the unreacted $K_4[Ru(CN)_6]$ was separated from the mixture and the filtered solution was evaporated to dryness. The solid was redissolved in 5 mL of water, reprecipitated with 200 mL of acetone, filtered off, and dried over P_4O_{10}. The solid thus obtained was treated by ion exchange chromatography using a column (3 × 10 cm) loaded with QAE-Sephadex A-25 and eluting the complex with 0.2 M NaI. The last fraction was concentrated to 3 mL and precipitated with 100 mL of cold EtOH to obtain a bright orange-brick powder. Yield: 60 mg (12%). The complex was dried under vacuum over P_4O_{10}. Anal. Calcd: C, 29.9; H, 2.9; N, 23.3. Found: C, 29.8; H, 3.1; N, 23.4.

(b) $K_2[Os(bpy)(CN)_4]\cdot 4H_2O$. The procedure was similar to the one described above. $K_4[Os(CN)_6]$ was prepared similarly to $K_4[Ru(CN)_6]$,[16] starting from OsO_4. During the irradiation of the hexacyanide complex, a broad absorption band was observed near 800 nm, suggesting the formation of mixed-valence species. Ascorbic acid was added in order to increase the yield of the reaction. Unreacted $K_4[Os(CN)_6]$ was not found after the irradiation. The purification procedure was like the one described above, using acetone instead of EtOH at the final precipitation step, the osmium complex being completely soluble in the latter solvent. Alternatively, the solution was loaded into a column (40 cm × 6 cm diameter) of Sephadex G-25 and the last fraction was collected. The volume was reduced to 5 mL, and a dark red precipitate was obtained after adding 50 mL of 1:1 ether−acetone. The solid was filtered onto a polyamid membrane of 0.2 μm pore size and dried under vacuum over P_4O_{10}. Anal. Calcd: C, 27.98; H, 2.66; N, 13.99. Found: C, 26.11; H, 2.51; N, 14.11.

The tetrabutylammonium salts were obtained by exchanging Na^+ (K^+) by Bu_4N^+ in a SP-Sephadex C-25 column, previously equilibrated with Bu_4NBr.

Instrumentation and Techniques. The solvents used for electrochemical and spectroscopic measurements were reagent grade reagents (except otherwise indicated), dried over molecular sieves and used without further purification. Acetone, acetonitrile, methanol, and dimethylformamide (DMF) were of spectroscopic grade and were used as supplied.

IR spectra were recorded as KBr pellets on Perkin-Elmer 983G and Nicolet 150P FTIR spectrophotometers. Some measurements were also performed in nonaqueous solutions (methanol, DMF, acetone) in the C−N stretching region. Shimadzu UV-160A and a Hewlett-Packard 8452A spectrophotometers were used to obtain the UV−visible spectra. The electrochemical measurements (cyclic and square-wave voltammetries) were performed in a standard three-electrode cell with a platinum wire as a working electrode and 0.1 M Bu_4NPF_6 as supporting electrolyte. The measurements were made against the saturated sodium chloride calomel electrode (SSCE) at 20 ± 2 °C. A PAR 273A potentiostat was used, controlled by a PC and the M270 software.

Emission spectra were recorded in different solvents on a Perkin-Elmer LS5 spectrofluorometer. Spectra recorded at 77 K were obtained in EtOH−MeOH (1/3) and in 9 M LiCl glasses, immersed in liquid nitrogen. Emission quantum yields in water at 23 ± 1 °C were determined by comparing the integrated emission spectra of the complexes relative to that of a solution containing $Ru(bpy)_3^{2+}$ (ϕ_{em} = 0.042) and having the same absorbance. Emission lifetimes were determined by laser flash photolysis using a pulsed nitrogen laser (Laseroptics LN2-004) as the excitation source (pulse ≈ 3 ns). The emission intensity (I_{em}) following the excitation was monitored at right angles to the laser pulse as a function of time. The voltage vs time signal was acquired with a Hewlett-Packard 54502A digital oscilloscope. Lifetimes were obtained by least-squares analysis of first-order decay plots of ln I_{em} vs time.

The basicities of coordinated cyanides were estimated through spectrophotometric titration experiments.[17] The solutions contained a fixed concentration of $[M(L\text{-}L)(CN)_4]^{2-}$ (ca. 10^{-5} M) and different concentrations of HCl (diluted solutions were used in order to avoid the precipitation of the protonated species); the ionic strength was fixed at 1 M with NaCl. The spectra were recorded between 250 and 600 nm, by using a quartz cell of 10 cm path length. The data were treated according to the NIPALS procedure;[18] thus, the absorbance matrix (the absorbance as a function of wavelength and pH) was decomposed into a product of target and projection matrices; using a suitable chemical

(16) Krause, R. A.; Violette, C. *Inorg. Chim. Acta* **1986**, *113*, 161.

(17) Indelli, M. T.; Bignozzi, C. A.; Marconi, A.; Scandola, F. In *Photochemistry and Photophysics of Coordination Compounds*; Yersin, H., Vogler, A., Eds.; Springer-Verlag: Berlin, Heidelberg, 1987; p 159.

(18) Kubista, M.; Sjöback, R.; Albinsson, B. *Anal. Chem.* **1993**, *65*, 994.

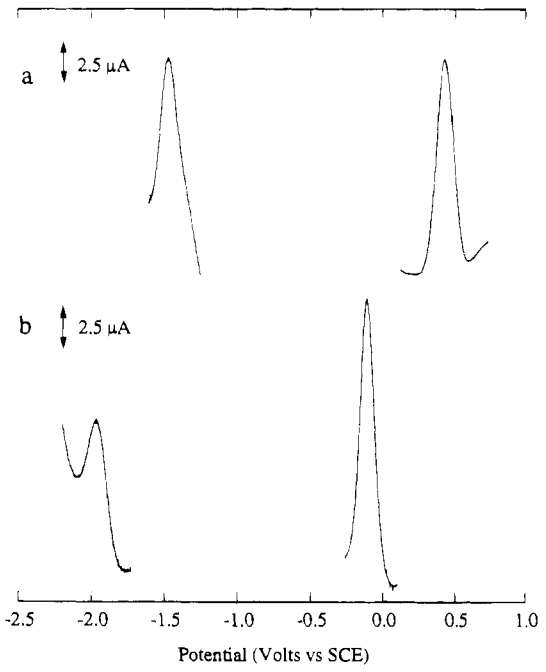

Figure 1. Square-wave voltammograms of (a) $[Ru(bpz)(CN)_4]^{2-}$ and (b) $[Os(bpy)(CN)_4]^{2-}$ in DMF solution (0.1 M Bu_4NPF_6). Conditions: square-wave amplitude (E_{sw}), 25 mV; frequency, 60 Hz; scan increment, 2 mV. The concentrations of electroactive species were ca. 1×10^{-4} M.

model, these matrices could be transformed into the concentration profile and the spectra of all the involved species. Assuming the reversible equilibrium $A + H^+ \rightleftharpoons AH^+$, and employing standard nonlinear least-squares fitting methods, the value of the equilibrium constant, K_a, as well as the spectra of A and AH^+ were obtained. The calculated spectrum of A was identical to the one measured at pH 7.0; the spectrum of AH^+ was consistent with that expected for a cyanide–monoprotonated species; *i.e.*, the maximum was shifted to higher energies.[19]

Results and Discussion

(a) UV–Visible Spectra, IR Spectra, and Electrochemistry. Band Energies and $E°$ values. Table 1 shows the electronic spectral results (energy maxima, molar absorbances, and assignments) for $[Ru(bpz)(CN)_4]^{2-}$ and $[Os(bpy)(CN)_4]^{2-}$ in aqueous and in organic solvent solutions. Figure 1 shows the square-wave voltammograms (SWV) for both complexes, in DMF; in each case, two peaks were detected, corresponding to redox reactions centered at the metal and the chelating ligand (E_{ox} and E_{red}, respectively; Table 2).[20] **(i) The $[Ru(bpz)(CN)_4]^{2-}$ ion.** The major absorptions in the visible region (Table 1, Figure 2) correspond to MLCT transitions from $d\pi(Ru)$ to the two lowest lying orbitals, π^*_1 and π^*_2 (bpz). The differences in energy, ca. $(6.5–7.0) \times 10^3$ cm^{-1}, compare well with those

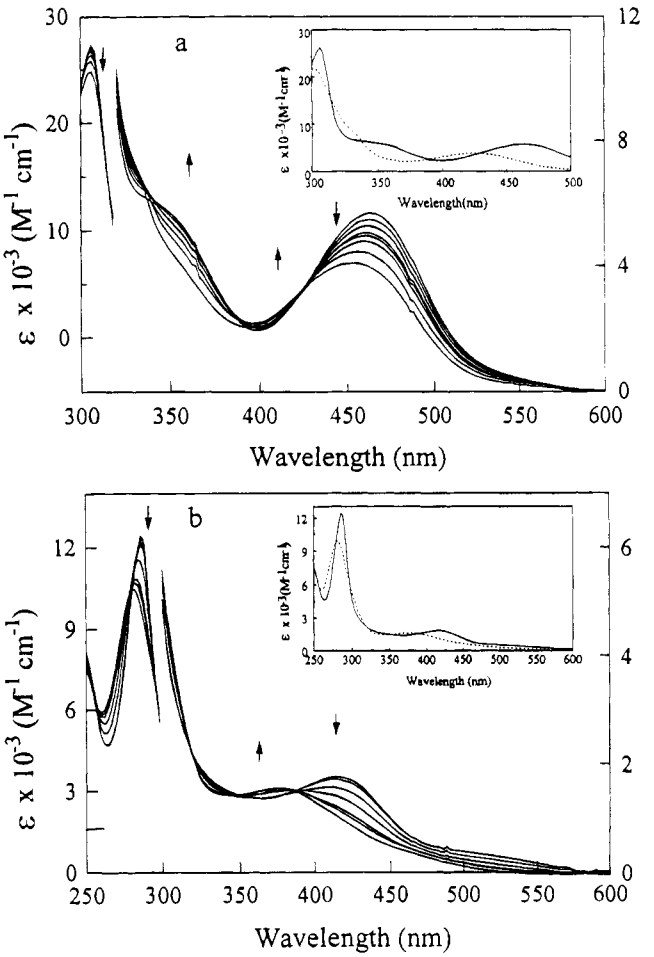

Figure 2. (a) Visible absorption spectra of $[Ru(bpz)(CN)_4]^{2-}$ in aqueous solution for different pH's. Arrows indicate decreasing pH (3.1, 1.8, 1.5, 1.3, 1.2, 1.1, 0.9, 0.7). Inset: Calculated spectra of $[Ru(bpz)(CN)_4]^{2-}$ (continuous line) and of protonated $[Ru(bpz)(CN)_4H]^-$ (broken line). (b) As (a) for $[Os(bpy)(CN)_4]^{2-}$, including inset. pH values: 3.6, 3.2, 2.8, 2.4, 1.9, 1.7, 1.5.

found in other Ru(II)–bpz complexes.[12] The UV bands are assigned to intraligand (IL) transitions, $\pi \rightarrow \pi^*_1$ and $\pi \rightarrow \pi^*_2$ (bpz).[12] The energies are almost solvent independent. An additional band was observed at ca. 200 nm, corresponding to $d\pi(Ru) \rightarrow \pi^*(CN)$ MLCT, as found previously for related complexes.[21]

The energy of the first MLCT transition (E_{op}) can be related to the measured potentials for the metal-based ($Ru^{III/II}$) and ligand-based, (L-L/L-L^-) couples through eq 1.[22]

$$E_{op} = (E_{ox} - E_{red}) + C \qquad (1)$$

The data in Table 2 (in DMF) show a good agreement with eq 1, with $C = 0.1$ eV. Upon inclusion of data for other members of the $[Ru(bpz)X_4]^{2+}$ series (X = bpy, bpz), an

(19) Toma, H. E.; Malin, H. E. *Inorg. Chem.* **1973**, *12*, 1039.

(20) (a) Christie, J. H.; Turner, J. A.; Osteryoung, R. A. *Anal. Chem.* **1977**, *49*, 1899. (b) O'Dea, J. J.; Osteryoung, J. G.; Osteryoung, R. A. *Anal. Chem.* **1981**, *53*, 695. In SWV, the reversible behavior is characterized by the coincidence of peak potentials upon forward and backward scanning, as well as by a value of 100 mV for the half-wave amplitude, $\Delta w_{1/2}$, when the experiment is performed using a square-wave amplitude, E_{sw}, of 25 mV. In our results, the difference between the peaks observed in the forward and backward scans was 6 mV for E_{ox} and 20 mV for E_{red}. The values of $\Delta w_{1/2}$ were 120 and 140 mV for E_{ox} and E_{red}, respectively. Both types of results correspond to a quasi-reversible behavior and are consistent with complementary cyclic voltammetric runs, showing a difference of 90 mV (instead of 60 mV) between the anodic and cathodic peak potentials. From the CV experiments the same $E_{1/2}$ values were obtained as those reported in Table 2 (SWV).

(21) Olabe, J. A.; Zerga, H. O.; Gentil, L. A. *J. Chem. Soc., Dalton Trans.* **1987**, 1267.

(22) Dodsworth, E. S.; Lever, A. B. P. *Chem. Phys. Lett.* **1986**, *124*, 152. A large body of data for the $[Ru(bpy)_2XY]^{n+}$ series (X, Y = general ligands, $n = 0–2$) can be interpreted through an equation closely related to (1): $E_{op} = \Delta E'(redox) + \chi_i + \chi_0$. In the latter, $\Delta E'(redox)$ is defined as a difference between E_{ox} and E_{red}, but the E_{red} value corresponds to the reduction of bpy in the field of Ru(III), in contrast with the experimentally obtained value of E_{red} in eq 1, which refers to a reduction in the field of Ru(II). Both values of E_{red} are connected through solvation terms, which are assumed to be constant in the series; thus, the constant C in eq 1 will include both solvation and reorganization terms.

Table 2. Electronic Absorption and IR Data, Electrochemical Results, and Photophysical Properties of $[M(L\text{-}L)(CN)_4]^{2-}$ Complexes (M = Fe, Ru, Os; L-L = bpy, bpz)

	$[Os(bpy)(CN)_4]^{2-}$	$[Ru(bpy)(CN)_4]^{2-}$ [a]	$[Fe(bpy)(CN)_4]^{2-}$ [b]	$[Ru(bpz)(CN)_4]^{2-}$	$Fe(bpz)(CN)_4]^{2-}$ [c]
$E_{op}(H_2O)$,[d] eV	2.99	3.10	2.57	2.68	2.18
E_{op}(DMF), eV	2.12	2.21		2.07	1.85[e]
$E_{ox}(H_2O)$,[f] V	0.47	0.78	0.30	1.00	0.57[e]
E_{ox}(DMF), V	−0.14	0.20	−0.24[g]	0.50	0.20[e]
E_{red}(DMF),[h] V	−1.98	−1.95		−1.48	−1.54[e]
$E_{ox} - E_{red}$(DMF), V	1.84	2.15		1.98	1.74
S_{op},[i] cm^{-1}/AN	180	140[j]	150	120	70
S_E,[k] V/AN	1.69	1.50	1.48	1.40	1.1
pK_a[l]	2.2	1.8[m]		0.55	
ν(CN), cm^{-1}	2091, 2053, 2035,[n] 2017	2092, 2060, 2048,[n] 2035[j]	2080, 2053, 2040,[n] 2030[o]	2105, 2073, 2066,[n] 2052	2094, 2073, 2065,[n] 2026
$E_{em}(H_2O$, 298 K), eV	1.81	2.03		1.76	
E_{em}(9 M LiCl, 77 K), eV	2.14	2.38		2.07	
E_{em}(MeOH/EtOH, 77 K), eV	1.91	2.18		1.88	
$\tau(H_2O$, 298 K), ns	3	101		5	
ϕ_{em}	<0.0005	0.0069		<0.001	
$E^{o'}(Os^{III/II*})$, aq, V[p]	−1.67	−1.60		−1.07	
$E^{o'}(Os^{III/II*})$, DMF, V[q]	−1.77	−1.83		−1.06	
$E^{o'}(Os^{II*/I})$, DMF, V[r]	−0.35	+0.08		+0.08	

[a] Reference 2, unless otherwise indicated. [b] Reference 25, unless otherwise indicated. [c] Reference 24, unless otherwise indicated. [d] E_{op} corresponds to the low-energy, singlet MLCT transition. [e] Katz, N. E. Work in progress. [f] E_{ox} is the potential of the $M^{III/II}$ couple (*vs* SSCE). [g] In Acetonitrile. [h] E_{red} is the potential of the ligand-based couple. [i] Slope of the plot of E_{op} *vs* AN. [j] Reference 8. [k] Slope of E_{ox} *vs* AN. [l] Corresponding to $[M(HNC)(CN)_3(L\text{-}L)]^- \leftrightarrow [M(CN)_4(L\text{-}L)]^{2-} + H^+$. [m] Reference 17. [n] Most intense peak. [o] Reference 29. [p] Calculated from $E_{ox} - E_{em}(o\text{-}o)$; an upper limit was estimated for $E_{em}(o\text{-}o)$, taken equal to E_{em}(9 M LiCl, 77 K). [q] Calculated as before; the $E_{em}(o\text{-}o)$ value in DMF was estimated by subtracting 0.51 V from the corresponding E_{em} values in 9 M LiCl at 77 K, assuming a behavior similar to that of $[Ru(bpy)(CN)_4]^{2-}$ (cf. ref 2). [r] Calculated from $E_{red} + E_{em}(o\text{-}o)$.

excellent linear plot with unit slope is obtained ($C = 0.2$ eV).[23] Besides, eq 1 is also well-behaved with data obtained for the $[Fe(bpz)(CN)_4]^{2-}$ [24] and $[Ru(bpy)(CN)_4]^{2-}$ ions.[2]

(ii) The $[Os(bpy)(CN)_4]^{2-}$ ion. The spectrum of $[Os(bpy)(CN)_4]^{2-}$ in aqueous solution (Figure 2) shows an intense band in the visible region, with a weaker component occurring at ca. 5000 cm^{-1} lower energy. Both can be assigned to MLCT transitions to excited states (π^*_1, bpy), predominantly singlet and triplet in character, respectively. On the basis of the comparable intensities, we assume that a considerable mixing exists between the spin states.[6]

The value of E_{op} for the singlet MLCT band of $[Os(bpy)(CN)_4]^{2-}$ (in DMF) also agrees with eq 1, with C = 0.3 eV (Table 2). It also fits well in the linear plot of E_{op} against ($E_{ox} - E_{red}$) for the $[Os(bpy)X_4]^n$ series (X = das, dppm, bpy, py, Cl^-, etc.).[5,6]

The MLCT transition, $d\pi(Os) \rightarrow \pi^*_2$(bpy), is buried in the tail of the first IL transition in aqueous solution, but it is better resolved in the lower acceptor solvents. The triplet component of the latter transition can also be detected as a shoulder at ca. 5000 cm^{-1} lower energy. At higher energies, the second IL transition and the $d\pi(Os) \rightarrow \pi^*(CN)$ MLCT transitions are observed. The energies of both IL transitions are almost solvent-independent.

(b) Band Intensities. The intensities of the corresponding MLCT transitions in aqueous solutions, as measured by the molar absorbances, are higher for $[Ru(bpz)(CN)_4]^{2-}$ than for $[Ru(bpy)(CN)_4]^{2-}$.[2] This can be related to the degree of mixing between the ground- and excited-state wave functions and is an evidence of a stronger π-back-bonding from Ru(II) to bpz than to bpy. A similar comparison can be done with data from $[Fe(bpz)(CN)_4]^{2-}$ [24] and $[Fe(bpy)(CN)_4]^{2-}$.[25] The analysis of intensities was taken as a complementary support in the comparison of the higher π-acceptor ability of pyrazine (pz) over pyridine (py) in the pentacyano−L−ferrate(II) complexes.[19] On the other hand, the molar absorbances of the MLCT bands, as well as the band shapes, are very solvent-dependent for a given complex.

(c) Solvent Dependence of MLCT Energies and Oxidation Potential. The MLCT bands show solvatochromism, for both $[Ru(bpz)(CN)_4]^{2-}$ and $[Os(bpy)(CN)_4]^{2-}$; as the acceptor ability of the solvent is increased (measured by the Gutmann's acceptor number),[26] the energies are shifted to higher values. Figure 3 shows the plots of the low-energy MLCT band against the acceptor number (AN) for both compounds (similar plots can be obtained by plotting the energy of other MLCT bands). The values of the slopes, S_{op}, are shown in Table 2, together with data for related complexes.

The solvatochromism of the MLCT bands has been previously found for $[Ru(bpy)(CN)_4]^{2-}$ and other mixed cyanide complexes.[2,7,8] The magnitude of the shift depends on the number of coordinated cyanides, for a given solvent. The N-ends of cyanides act as electron donors in specific interactions with the solvent; thus, the π-electron density is drawn away from the metal and the energy of the HOMO is lowered, increasing the energy of the MLCT band. Consequently, E_{ox} increases as well, as shown in Figure 3. The slope, S_{op}, is lower for $[Ru(bpz)(CN)_4]^{2-}$ than for $[Ru(bpy)(CN)_4]^{2-}$. Bipyrazine is a weaker σ-donor (lower pK_a), as well as an expectedly stronger π-acceptor (lower energy of its LUMO) compared to bipyridine; hence, the basicity of cyanides should be lower in the first compound (see below), decreasing the sensitivity of the lone electron pair to solvent interactions. The slope values in the E_{ox} vs AN plots, S_E, show little discrimination, but the results are still consistent.

For $[Os(bpy)(CN)_4]^{2-}$, both S_{op} and S_E values are the greatest among complexes in Table 2. This is consistent with the strong

(23) Rillema, D. P.; Allen, G.; Meyer, T. J.; Conrad, D. *Inorg. Chem.* **1983**, *22*, 1617.
(24) Katz, N. E. *An. Asoc. Quim. Arg.* **1991**, *79*, 67.
(25) (a) Schilt, A. A. *J. Am. Chem. Soc.* **1960**, *82*, 3000. (b) Toma, H. E.; Takasugi, M. S. *J. Solution Chem.* **1983**, *12*, 547. (c) Winkler, J. R.; Creutz, C.; Sutin, N. *J. Am. Chem. Soc.* **1987**, *109*, 3470.
(26) (a) Gutmann, V. *The Donor-Acceptor Approach to Molecular Interactions*; Plenum: New York, 1980. (b) Marcus, Y. *Chem. Soc. Rev.* **1993**, 409.

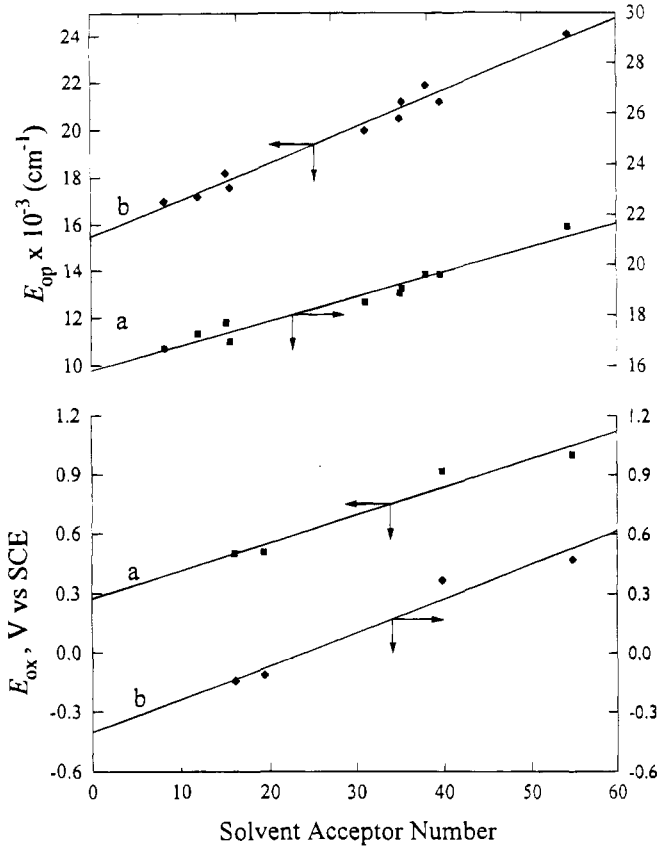

Figure 3. Dependencies of the absorption band maximum, E_{op}, for the MLCT transition (upper plots) and of the $M^{III,II}$ potential, E_{ox} (lower plots), on solvent acceptor number (Gutmann's scale): (a) $[Ru(bpz)(CN)_4]^{2-}$; (b) $[Os(bpy)(CN)_4]^{2-}$.

π-donor ability of Os(II), which places a higher electronic density on cyanides.[10]

(d) pH Effects. Relative Basicities of Coordinated Cyanides. An extreme case of donor–acceptor interactions of coordinated cyanides is given by the protonation at the nitrile end in aqueous solution. Figure 2 shows the spectra obtained by lowering the pH of solutions of $[Ru(bpz)(CN)_4]^{2-}$ and $[Os(bpy)(CN)_4]^{2-}$. The MLCT bands shift to higher energies, showing well-defined isosbestic points. The shifts can be interpreted in terms of the stronger π-acceptor ability of the CNH ligand compared to aqueous cyanide, which stabilizes the HOMO and increases the energy of the $d\pi(M) \rightarrow \pi^*(L\text{-}L)$ transition. The decrease in intensity of the MLCT band in the calculated spectrum of the protonated complex compared to the unprotonated one means that CNH is competing for the π-electron density with the chelating ligand more effectively than aqueous cyanide does.

The lower pK_a for the $[Ru(bpz)(CNH)(CN)_3]^-$ ion, 0.55,[27] compared to the bpy analogue, 1.8 (Table 2), is consistent with bpz being a weaker σ-donor and stronger π-acceptor than bpy. The pK_a values of coordinated cyanides were also employed as a complementary probe of the π-acceptor ability of the L ligand in the series of pentacyano–L–ferrate(II) complexes; in that case, the value for L = pz, 1.9,[19] was lower than that for L = py, 2.1. Finally, the highest pK_a value for $[Os(bpy)(CN)_4]^{2-}$, 2.2, is consistent with all the previous discussion.

(e) Infrared Spectra. Table 2 shows the stretching wavenumbers, ν(CN), for $[Ru(bpz)(CN)_4]^{2-}$, $[Os(bpy)(CN)_4]^{2-}$, and related complexes. Four bands are observed, as expected from C_{2v} symmetry; this was also found for $[Fe(bpy)(CN)_4]^{2-}$,[29] $[Fe(bpz)(CN)_4]^{2-}$,[24] and tetracarbonyl–diimine complexes of Mo and W.[14] The ν(CN) values for $[Ru(bpz)(CN)_4]^{2-}$ are greater than those for $[Ru(bpy)(CN)_4]^{2-}$, as for the corresponding carbonyls. Although the differences are small, they seem to be significant and can be attributed, again, either to a weaker σ-donor or to a stronger π-acceptor ability of bpz compared to bpy.

It can also be seen that ν(CN) for $[Os(bpy)(CN)_4]^{2-}$ has the lowest value. By considering all types of bonding interactions being stronger in osmium because of a better overlap with cyanide orbitals, we conclude that the stronger σ-influence, leading to an increase in ν(CN), is more than compensated by the π-interactions (both types, acceptor and donor, should act in the sense of decreasing ν(CN)). On the other hand, ν(CN) appears to be independent of the solvent; this is a remarkable result, considering that the π-acceptor ability of cyanide decreases in solvents of low acceptor number and, therefore, an increase in ν(CN) should be expected. We conclude that a stronger π-donor ability of cyanide toward the metal center compensates for the decrease in π-acceptor ability.

(f) Ligand Reduction Potentials: Competitive Back-Bonding Effects. The E_{red} values for $[Ru(bpz)(CN)_4]^{2-}$ and $[Os(bpy)(CN)_4]^{2-}$ complexes (Table 2) are highly negative, near the corresponding values for the free ligands (−1.66 and −2.18 V, in DMF, respectively).[15] In the series of $[Ru(bpz)X_4]^n$ and $[Os(bpy)X_4]^n$ complexes, the E_{red} values are, in general, positively shifted by ca. 0.6–1.0 V compared to the free-ligand values.[5,6,12] The energy of the π^*(L-L) level decreases upon coordination, but this can be counterbalanced by the interaction between $d\pi$(M) and π^*(L-L). In agreement with the IR results, the E_{red} values indicate that the $M(CN)_4$ moieties behave as strong π-donors toward the L-L ligands when the complexes are dissolved in weak-acceptor solvents such as DMF or acetonitrile.

(g) Photophysical Properties. Emission and absorption maxima and excited-state photophysical properties are displayed in Table 2 for $[Ru(bpz)(CN)_4]^{2-}$, $[Os(bpy)(CN)_4]^{2-}$, and related complexes, in water and DMF solutions. No emission was detected in organic solvents at room temperature.

Upon comparison with data for the $[Ru(bpz)X_4]^n$ and $[Os(bpy)X_4]^n$ series, the results in Table 2 fit well in the linear plots of E_{em} against E_{op} or against $(E_{ox} - E_{red})$. Thus, we can assign the emissions as being from $d\pi(Ru,Os) \rightarrow \pi^*$(bpz, bpy) MLCT excited states. On the other hand, the excitation spectra resemble the absorption spectra, showing that the singlet excited states decay rapidly to the triplet excited states.

The emissions are substantially blue-shifted at low temperatures, as previously found for $[Ru(bpy)(CN)_4]^{2-}$. The solvent dependence of emission is smaller than the solvent dependence of the absorption, consistent with the lower basicity of the cyanide ligands in the excited state.

The potentials of the excited-state couples, $E^{o\prime}$, were estimated as detailed in Table 2. The excited-state complexes are much less powerful oxidants than the corresponding M(III) complexes but are very strong reductants, slightly weaker than the reduced

(27) The measured pK_a is in fact a mixed value, because of the availability of two sites for simultaneous protonation. If protonation occurred at the N-exposed end of bpz, the MLCT band should be shifted to lower energies,[14] which is not the case. From the observed energy shift and good isosbestic point, we conclude that protonation at cyanide is highly predominant. Although the pK_a of free bpz is 0.45, the pK_a of coordinated bpz could be significantly lower than zero (−2.2 in $Ru(bpz)_3^{2+}$ for the first protonation),[28] due to the inductive effects associated with coordination, probably not sufficiently compensated by π-back-donation from Ru(II) to bpz. In fact, we did not detect any spectral evidence of protonation on bpz down to pH 0.

(28) Crutchley, R. J.; Kress, N.; Lever, A. B. P. *J. Am. Chem. Soc.* **1983**, *105*, 1170.

(29) Schilt, A. *Inorg. Chem.* **1964**, *3*, 1323.

ground-state complexes. Either $E^{\circ\prime}(Os^{III/II*})$ or $E^{\circ\prime}(Os^{II*/I})$ values fit well in the linear plots against the corresponding E_{ox} values for the $[Ru(bpz)X_4]^n$ and $[Os(bpy)X_4]^n$ series. The lifetimes and quantum yields are the shortest and the lowest, respectively, by comparison with other complexes of the corresponding $[M(L\text{-}L)X_4]^n$ series. As with $E^{\circ\prime}$, the tendencies in both properties can also be traced to the E_{ox} values. In the limit of low emission energies, $\tau = 1/k_{nr}$; thus, the significantly shorter lifetimes for $[Ru(bpz)(CN)_4]^{2-}$ and $[Os(bpy)(CN)_4]^{2-}$ compared to $[Ru(bpy)(CN)_4]^{2-}$ can be explained by the energy-gap law, as well as by the influence of spin–orbit coupling in promoting a greater nonradiative deactivation rate for the osmium complex.[3]

The short lifetimes are not advantageous for $[Os(bpy)(CN)_4]^{2-}$ and $[Ru(bpz)(CN)_4]^{2-}$ behaving as good photosensitizers. On the other hand, they are both able to react as strong reductants in the excited state and are good absorbers in the visible region. Besides, photolabilization processes are absent, as expected for Os(II) complexes with high-lying dd states; remarkably, this is also the case for $[Ru(bpz)(CN)_4]^{2-}$. Both of the complexes could be used as building blocks in the design of more complex supramolecular entities, taking profit from the binding abilities of cyanides and the absorbing properties induced by the chelating ligand.

Acknowledgment. We thank the National Scientific Council (CONICET) and the Universities of Buenos Aires and Tucumán for support of this work. N.E.K. and J.A.O. are members of the scientific staff of CONICET. The aid of Prof. Pedro Aramendia in performing the laser flash photolysis experiments and valuable discussions with Leonardo Slep are gratefully acknowledged.

IC940371E